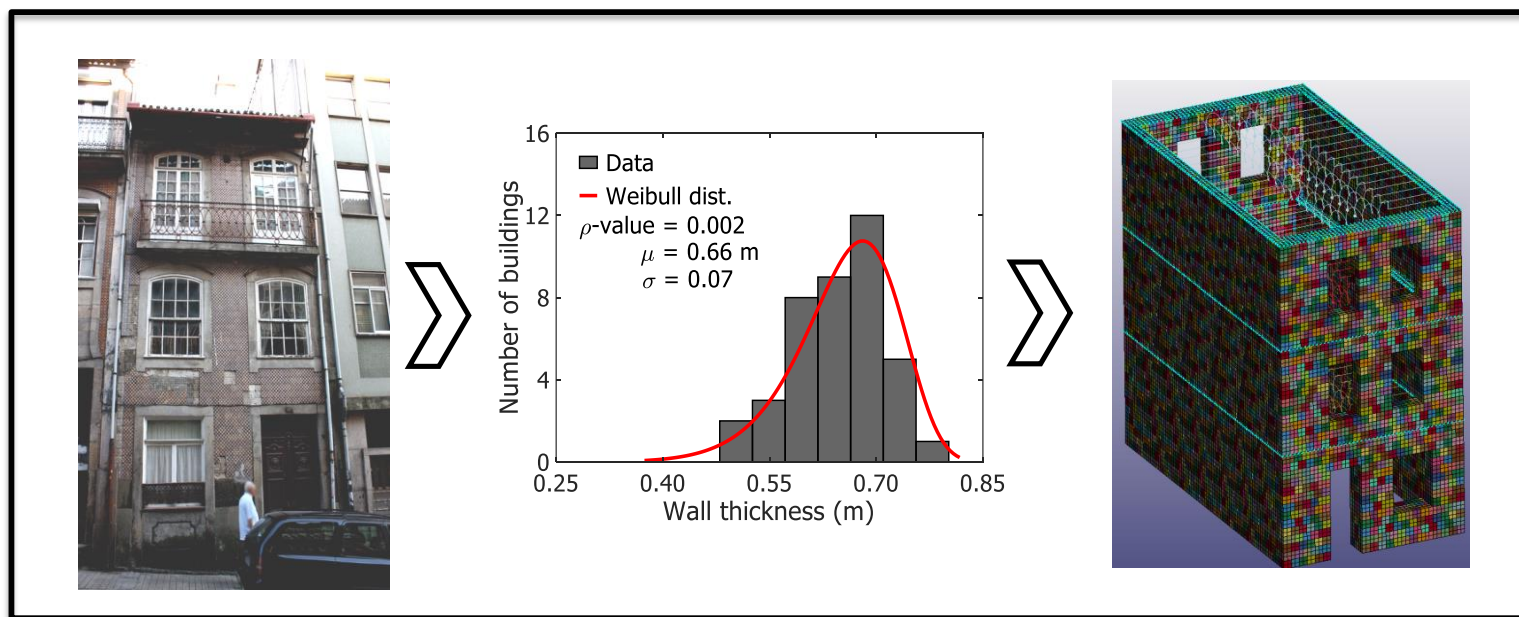


Exploring Benefit-Cost Analysis for Earthquake Risk Reduction

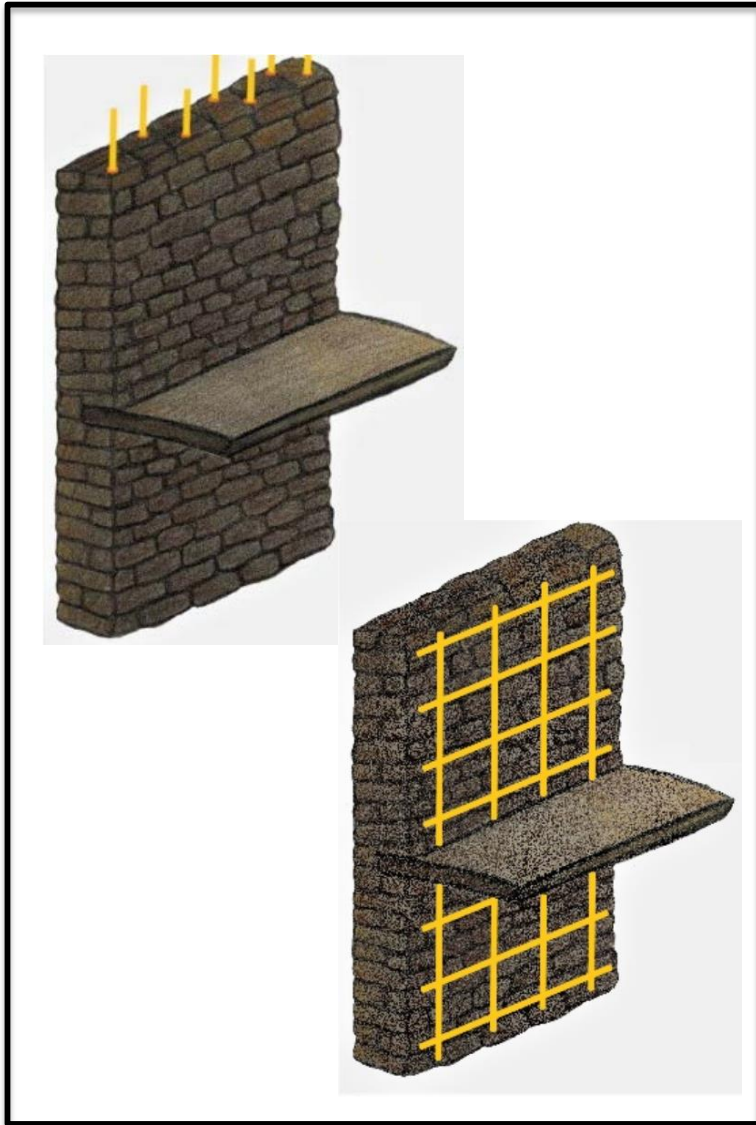
Holger Lovon (U Aveiro)

Supervision:

Vitor Silva (U Aveiro), Tiago Ferreira (U Minho), Romeu Vicente (U Aveiro)



The benefit-cost analysis consist on measuring whether the advantages of a programme are greater than its costs



Structural retrofitting reduces physical losses, this effect can be translated to a benefit-cost analysis framework.

However, including the reduction of potential human losses into the benefit cost-analysis framework can change the perspective of the outcomes, and eventually become the retrofitting more attractive.

Coburn et al. (1992) propose to correlate the earthquake fatalities with the extent of collapse (volume of debris)

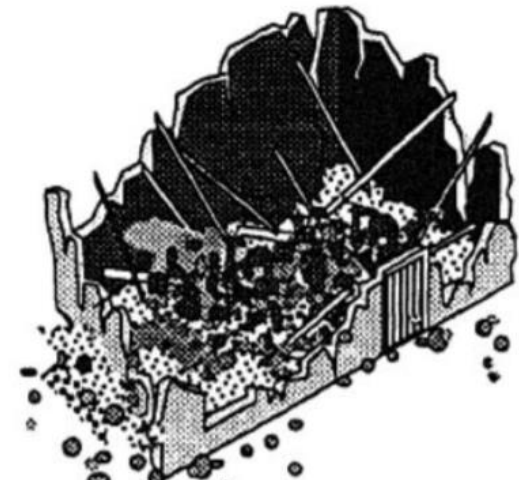
The figure illustrates a building in Damage State 5. Nevertheless, different volume of debris are reported in each case. The volume of debris is associated with the free space inside the building for survivors.



Damage Level: D5 Collapse
Extent of Collapse: 10% of Volume



Damage Level: D5 Collapse
Extent of Collapse: 50% of Volume



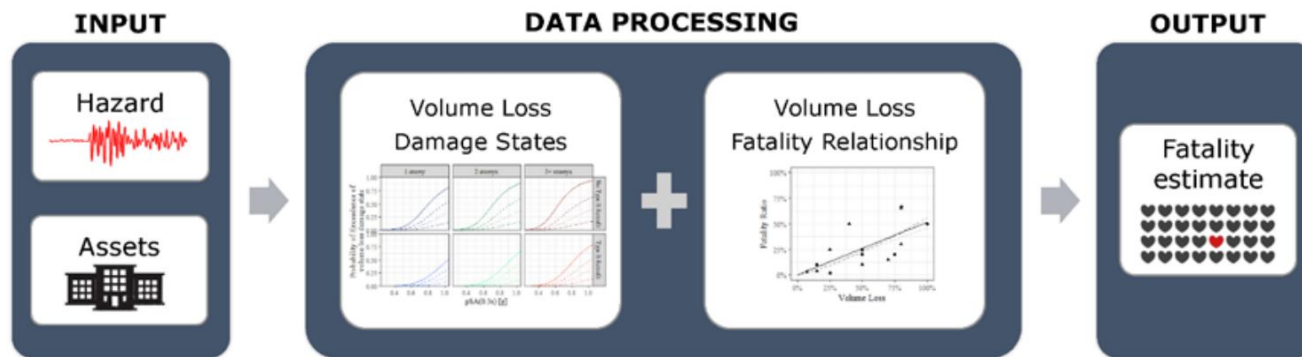
Damage Level: D5 Collapse
Extent of Collapse: 100% of Volume

Source: Coburn et al. (1992)

Fig. 2 Example of different extents of collapse for damage state 5 in masonry buildings

Abeling and Ingham (2020) proposed an empirical model to predict earthquake fatalities with volume loss

Empirical methods for human loss assessment requires extensive post-earthquake field data. This fact affects its feasibility in countries with moderate to low seismicity where important earthquakes did not take place in recent years, or places where field data was not properly collected.



Source: Abeling and Ingham (2020)

Fig. 2 Procedure proposed by Abeling and Ingham for fatality estimation

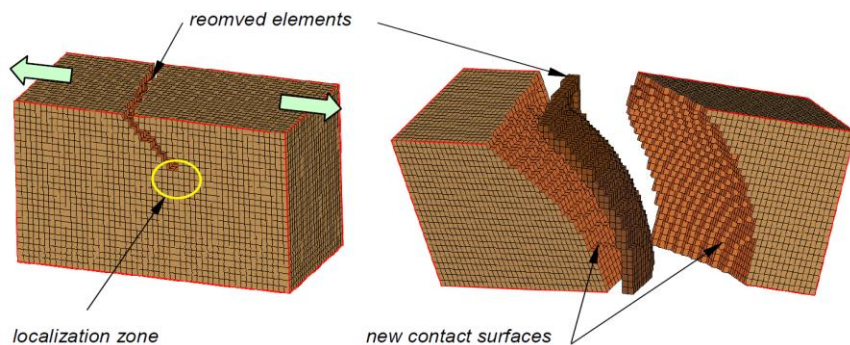
Therefore, mechanics-based approaches for human loss assessment is being recently addressed by researchers.

Analytical models have to be able to model explicitly the collapse of the building, hence the loss volume can be calculated.

Several techniques allow the collapse modelling, a revision of two techniques was made in this study

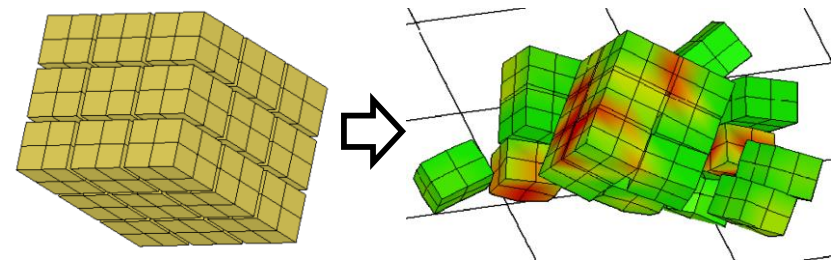
Erosion

Consist in the deletion of some elements once they achieve a given criteria. By eroding enough elements, one part is divided into two or more bodies



Contact surface

Consist in joining two parts through a contact surface. The contact surface is deleted for a given criteria and the two bodies are released



Source: Bakeer (2009)

Fig. 3 Techniques explored for collapse modelling of masonry buildings

LS-Dyna software was used to implement this techniques

LS – Dyna is a general-purpose finite element program characterized for its enriched capabilities for contact modelling.



Some of the most important advantages are listed below:

- The input data can be provided as text file
- Capable to model flexible body kinematics
- Modelling large deformations
- Developed explicitly for contact modelling



LS-Dyna



LS-Prepost

The erosion technique was implemented to model the collapse of a building tested at LNEC (Elk and Doornhof, 2015)

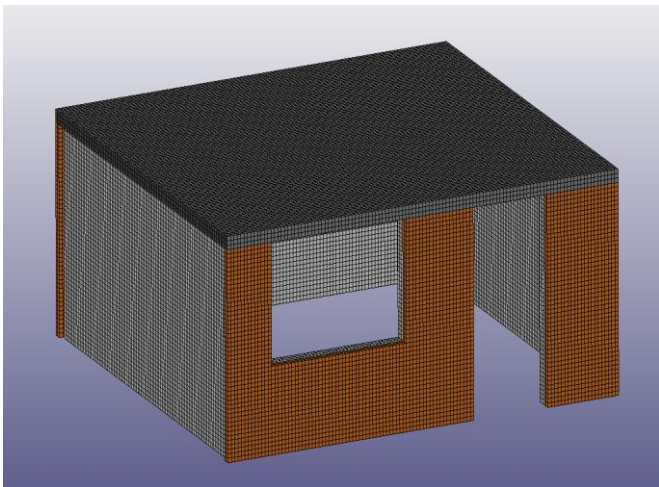


Fig. 4 Schemes of double leaf masonry building tested at LNEC

About the model

- 96 884 elements
- 10 minutes per 1 seconds of analysis approximately (4 processors 3.6 GHz)
- Two deletion criterions were establish in the model: Maximum principal strain at failure and shear strain at failure
- $E=1.4 \text{ GPa}$, $\sigma_t=1.05 \text{ MPa}$, $\tau = 0.85 \text{ Mpa}$
 $\varepsilon = 0.0025$

The contact modelling approach has two phases: before and after the failure

The tiebreak contact algorithm was used, it consist on attaching blocks using cohesive elements. The condition for the release is given by an ellipsoid failure surface of Normal and Tensile strength. The blocks are assumed to have an elastic behavior, therefore the inelastic behavior is concentrated in the contact surface. This is the first phase.

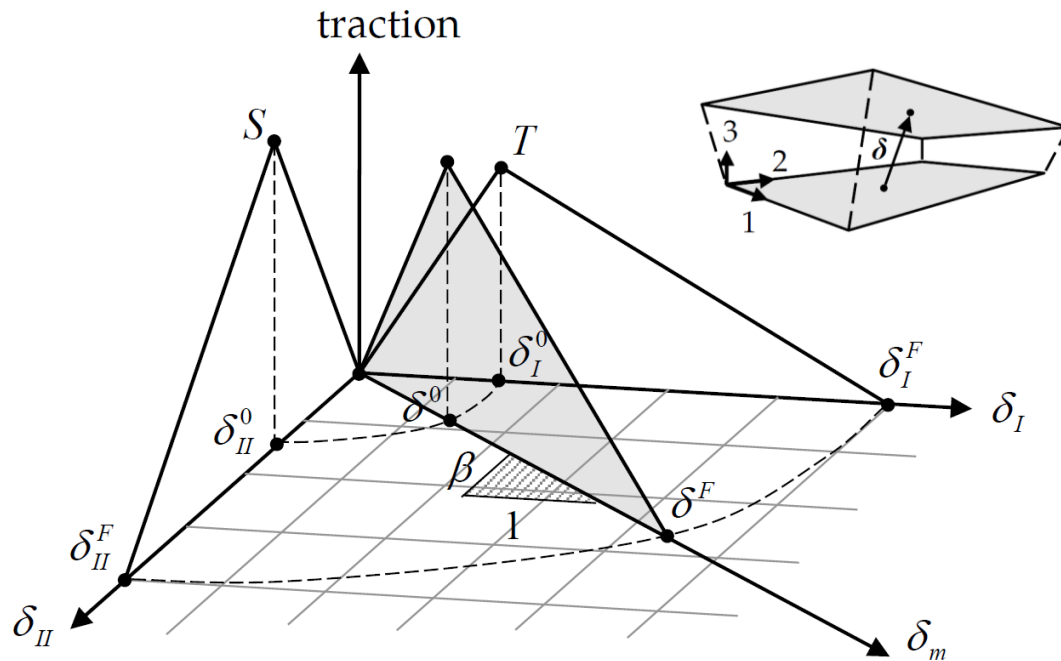


Fig. 5 Mixed-mode traction-separation law

$$\left(\frac{|\sigma_n|}{NFLS} \right)^2 + \left(\frac{|\sigma_s|}{SFLS} \right)^2$$

NFLS, Normal FaiLure Stress
SFLS, Shear FaiLure Stress

Source: LS-Dyna Manual II (2020)

The second phase consist in the analysis of the interaction between blocks

The contact forces are calculated under the penalty stiffness criterion. It consist on assessing a reaction force proportional to the penetration of the slave node on the master segment.

LS-Dyna algorithms make a two way analysis, it means that calculate the interaction forces swapping slave and master assignment.

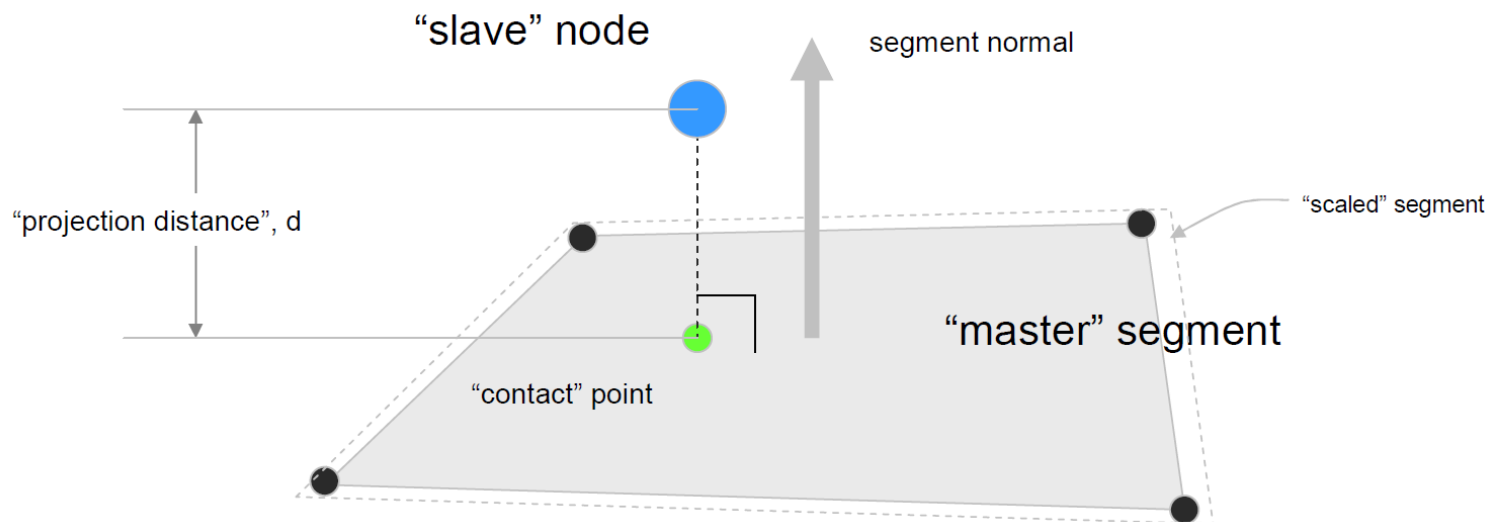
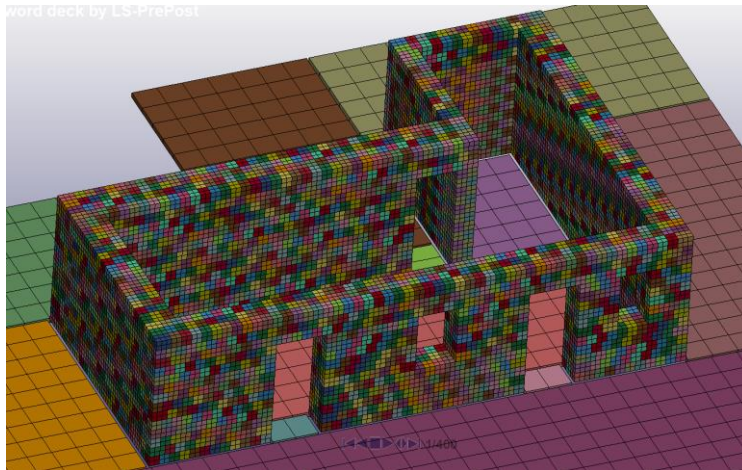


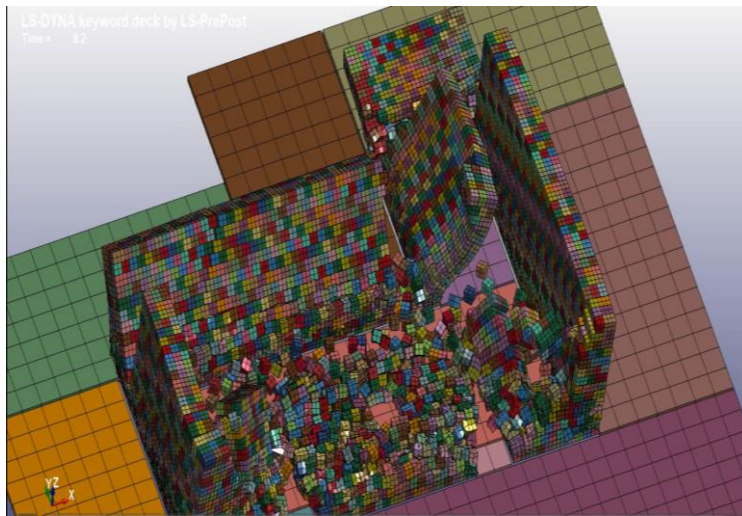
Fig. 6 Scheme of the penalty stiffness approach for contact modelling

Because the large number of parts that shape the model, a MatLab code was created to input the model as text file



About the model

- 6 464 parts – 53 826 elements
- 5 minutes per 1 seconds of analysis approximately (4 processors 3.6 GHz)
- $E=0.78$ GPa, $\sigma_t=0.15$ MPa, $\tau = 0.14$ MPa
 $\mu = 0.4 - 0.6$



About the code

- The code generates the building starting from an Excel spreadsheet which contains the building sizes
- An interlocking effect is emulated by shifting the parts in the horizontal plane

Fig. 7 Schemes of first limestone masonry building modelled within the contact approach

The purpose is to apply the selected technique to a building portfolio

The target population are limestone and granite Portuguese masonry buildings. The exposure model was updated using the Census data (INE 2011) at minimum available level.

Density maps were created for URM with and without concrete slab using Quartic Kernel density interpolation. The pixel size is 0.1 km and the search ratio is 1 km.

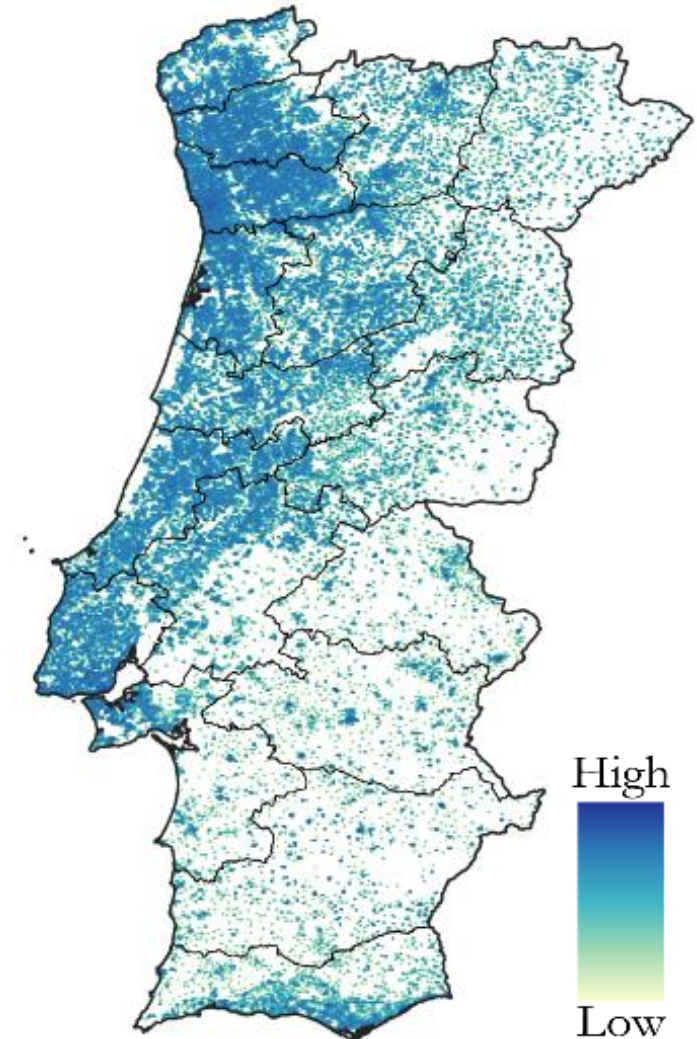


Fig. 8 Density map of URM buildings without RC slab

A cumulative exposure curve was calculated as part of the exposure model

In order to understand the seismic hazard to which the masonry building stock is exposed, the census database was crossed with the seismic hazard map proposed by Vilanova and Fonseca (2007) for a probability of exceedance of 10% in 50 years

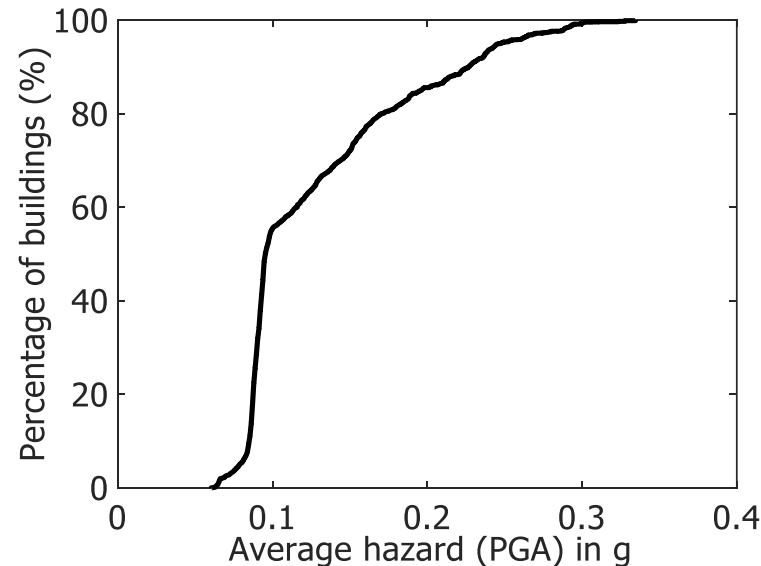


Fig. 9 Percentage of buildings exposed to different levels of seismic hazard expressed in terms of PGA (g)

The curve indicates that around 50% of the masonry building stock is exposed to at least 0.1 g PGA

Field data of limestone and granite buildings was obtained

NCREP consulting company provided access to its granite building database. Data for limestone masonry buildings was obtained from Vicente et al. (2011). Data from a total of 185 buildings was gathered.

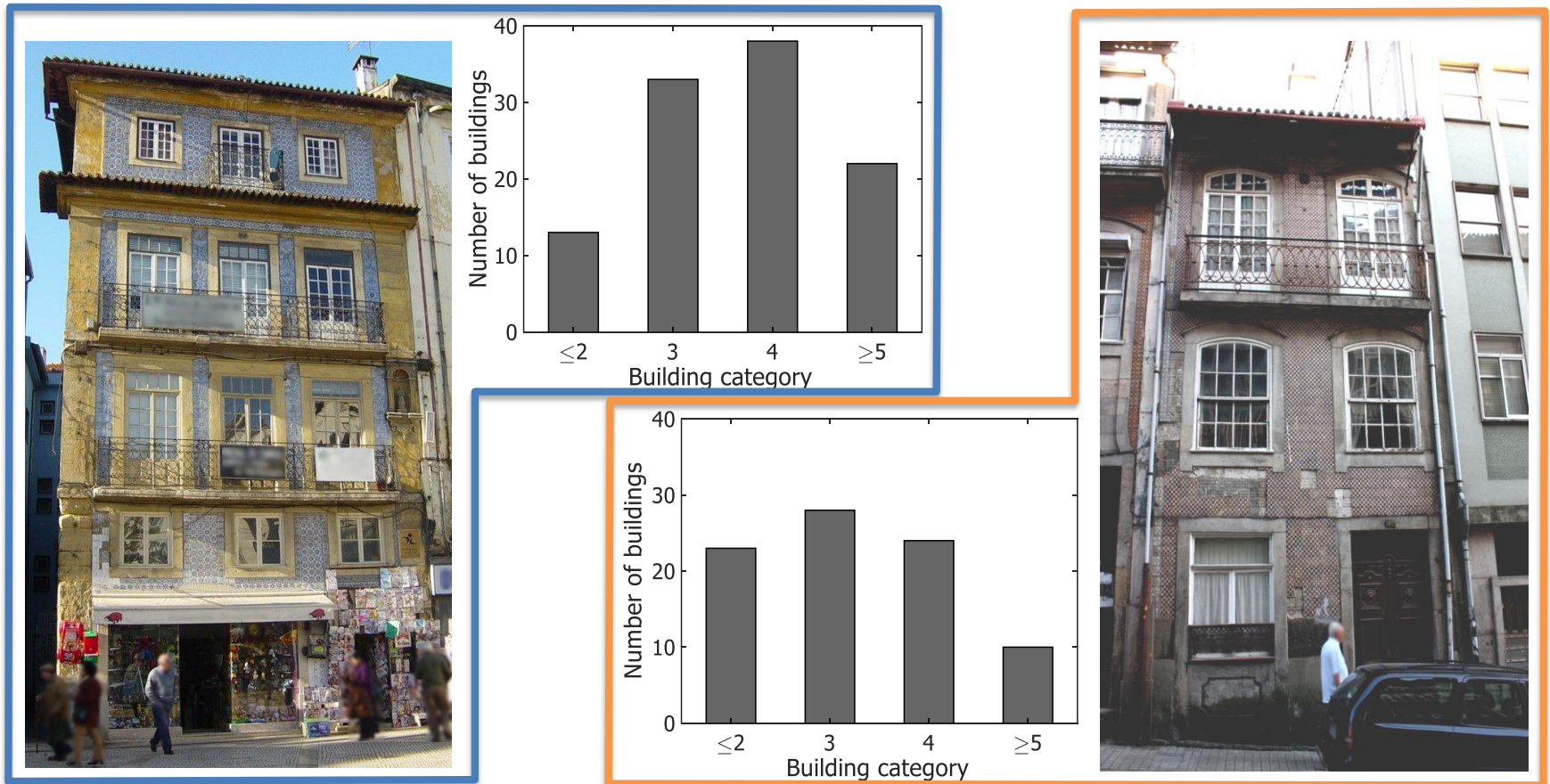


Fig. 10 Schemes and number of Limestone and granite buildings analyzed

Building features were modeled using probability density functions (Lovon et al. 2020)

The lack of data was overcome by grouping the data from different building categories. This procedure was validated using ANOVA analysis to explore significant statistical differences.

The ground floor height

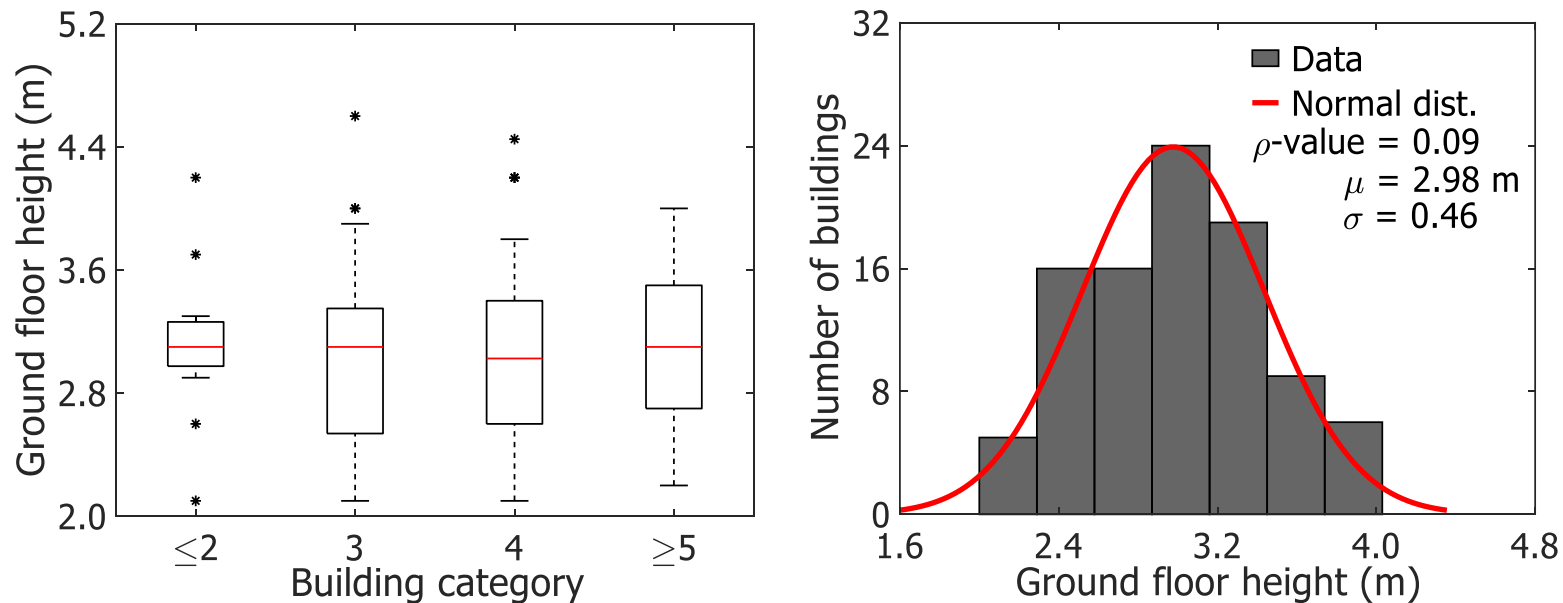


Fig. 11 Dispersion, Histogram, fitted distribution and goodness-of-fit results for the ground floor height of Limestone masonry buildings

Length of the building in the façade and the orthogonal direction

ANOVA analysis indicates that building category do not influence the building length, but there is a significant difference between lengths in both directions. Then each direction was modelled by separate, but building categories were grouped.

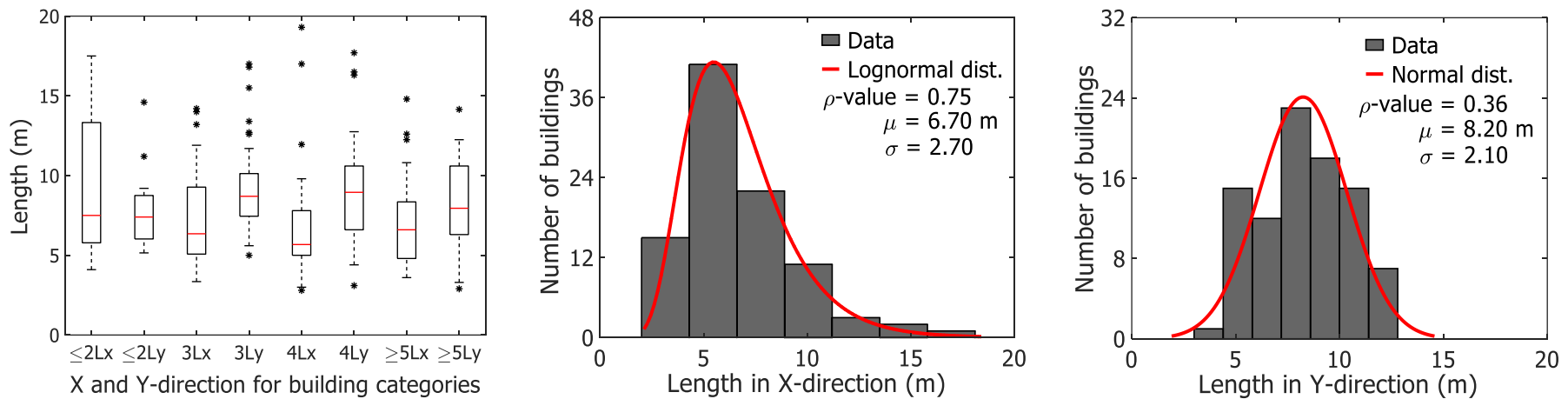


Fig. 12 Dispersion, Histogram, fitted distribution and goodness-of-fit results for the length in façade (X) and orthogonal (Y) direction in Limestone masonry buildings

Thickness of the walls in the ground storey

The thickness of the walls is directly related with the capacity to dissipate energy during a seismic event (Borzi et al. 2008). A significant difference was found between buildings of more than 3 storeys, then the data was grouped into two categories (≤ 3 and >3).

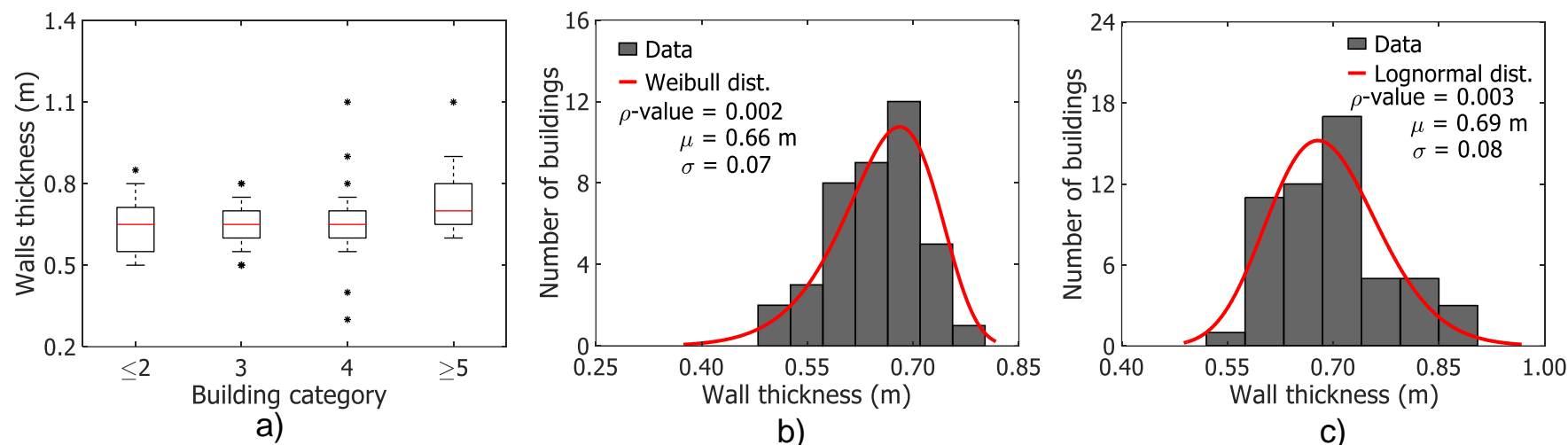


Fig. 13 a) Dispersion, b) and c) Histogram, fitted distribution and goodness-of-fit results wall thickness in ≤ 3 and >3 building categories respectively for Limestone masonry buildings

Reduction of wall thickness along the height

During the revision of the data, it was identified the reduction of wall thickness along the height, which can be seen in Fig. 14a. Then, the average reduction ratio was modelled for future sampling.

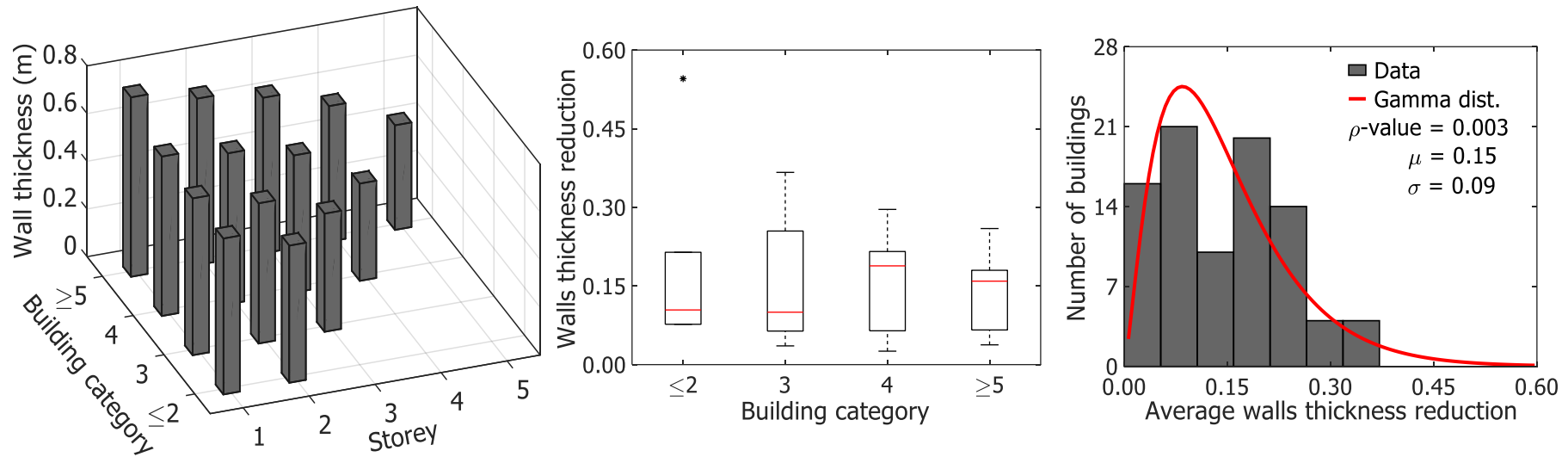


Fig. 14 a) Mean wall thickness of each storey per buildings height category, b) Dispersion of the mean thickness reduction, c) Histogram, fitted distribution and goodness-of-fit results for the mean wall thickness reduction

Other features like regular storeys height, ratio of openings and average density of non-structural walls were also modelled

Table 1. Random variables for limestone and granite masonry buildings

Random variable	Unit	Limestone			Granite		
		Function	Mean	Std. deviation	Function	Mean	Std. deviation
Ground floor height	m	Normal	2.98	0.46	Normal	3.60	0.39
Upper storeys height	m	Normal	2.90	0.31	Normal	3.30	0.39
Length X-direction	m	Lognormal	6.70	2.70	Lognormal	6.20	0.94
Length Y-direction	m	Normal	8.20	2.10	Normal	17.0	3.90
Wall thickness (≤ 3 storeys)	m	Weibull	0.66	0.07	Weibull	0.54	0.11
Wall thickness (> 3 storeys)	m	Lognormal	0.69	0.08	Normal	0.61	0.11
Average wall thickness reduction	-	Gamma	0.15	0.09	Gamma	0.16	0.08
Opening ratio (ground)	-	Beta	0.46	0.14	Beta	0.55	0.13
Opening ratio (upper storeys)	-	Beta	0.27	0.05	Beta	0.43	0.10
Non-structural walls density	-	Gamma	0.026	0.010	Gamma	0.026	0.010

A literature review of the mechanical properties of limestone and granite masonry buildings was also carried out.

Table 2. Existing studies that addressed the mechanical properties of limestone masonry in Portugal

Source	Elasticity modulus (GPa)	Compressive strength (MPa)	Shear strength (MPa)	Type of test	Masonry description
Pagaimo (2004)	0.30	1.00	-	In-situ flat-jack test	Irregular limestone masonry. Clay and lime mortar.
Pinho (2007)	0.31	0.43	-	Laboratory compression test	Irregular limestone masonry. Lime and sand mortar
Vicente (2008)	1.71	0.76	-	In-situ flat-jack test	Irregular limestone masonry. Lime, sand, pebble and clay mortar
Milosevic et al. (2013)	1.64	8.01	0.45	Laboratory uniaxial compression, and triplet shear test	Irregular limestone masonry. Hydraulic lime and sand mortar
	0.56	7.41	0.22		Irregular limestone masonry. Air lime and sand mortar
Moreira (2014)	1.02	1.70	0.29	Laboratory uniaxial, and diagonal compression test	Irregular limestone masonry. Hydraulic lime, sand, clay-rich sand and cement mortar
Simões (2016)	2.00	1.89	0.19	In-situ flat-jack test	Irregular limestone masonry. Air lime mortar – Pombalino Building.
	0.39	0.63	0.13		Irregular limestone masonry. Air lime mortar – Gaioleiro Building.

Three façade types were identified during the revision of the data

The process consist on sampling a ratio of openings. After, a façade configuration is selected based on a predefined range of application. The final step consist on selecting the opening sizes that better match the ratio of openings. Very low residuals were found during the process.

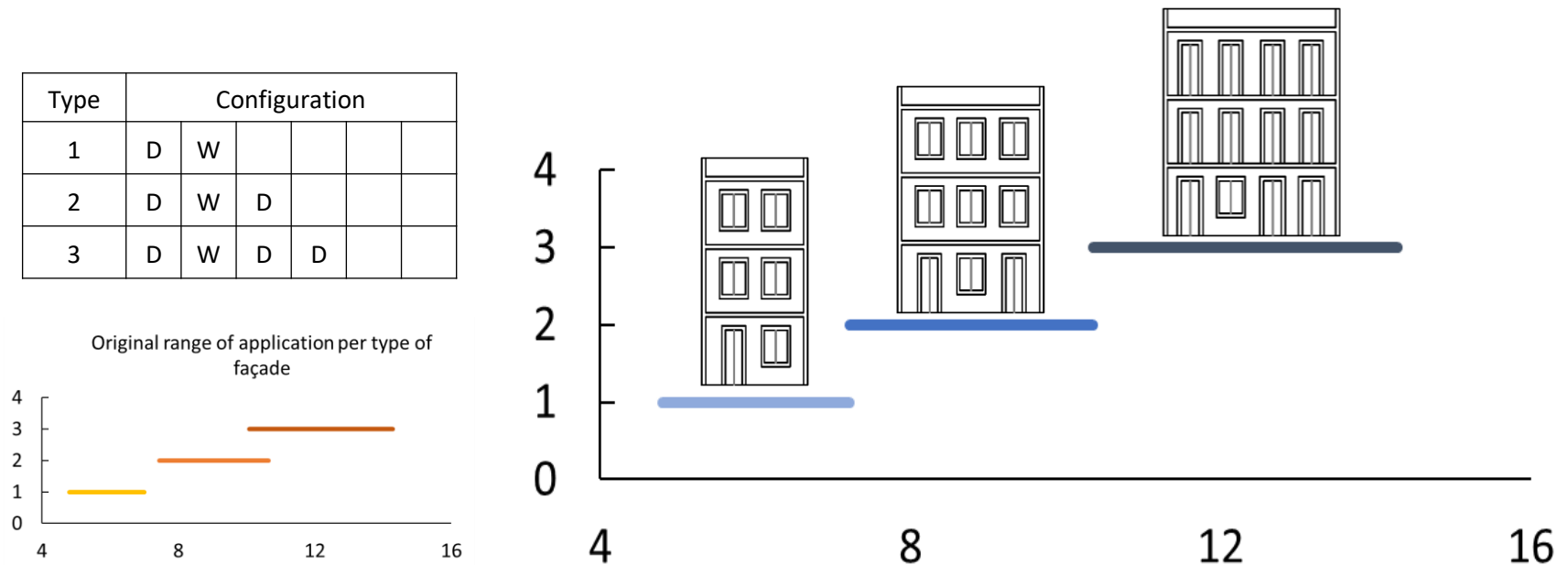


Fig. 15 Procedure for sampling of 3-storey buildings

The sampling procedure was implemented within a MatLab routine

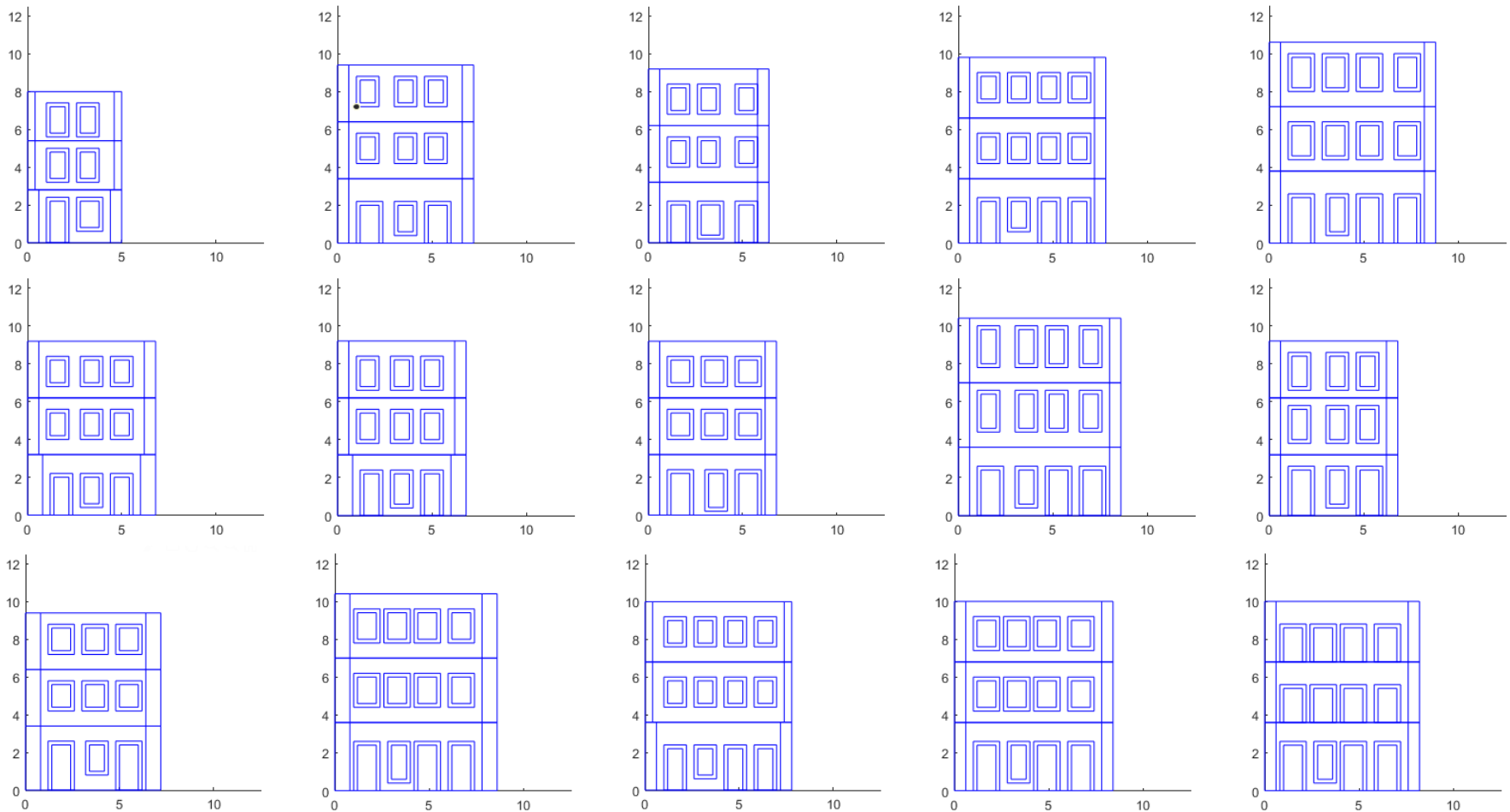


Fig. 16 Sample of 15 3-storey buildings randomly generated. Lengths in meters (m)

A third MatLab routine was implemented to transform the sample of buildings into LS-Dyna models

Some improvements were made for the generation of this models:

- Compression links to represent inter-storey timber joists
- Automatic deletion of elements that falls below the ground level
- Interlocking between walls
- Previous calibration of Pushover and Eigen-analysis
- Hourglass formulation

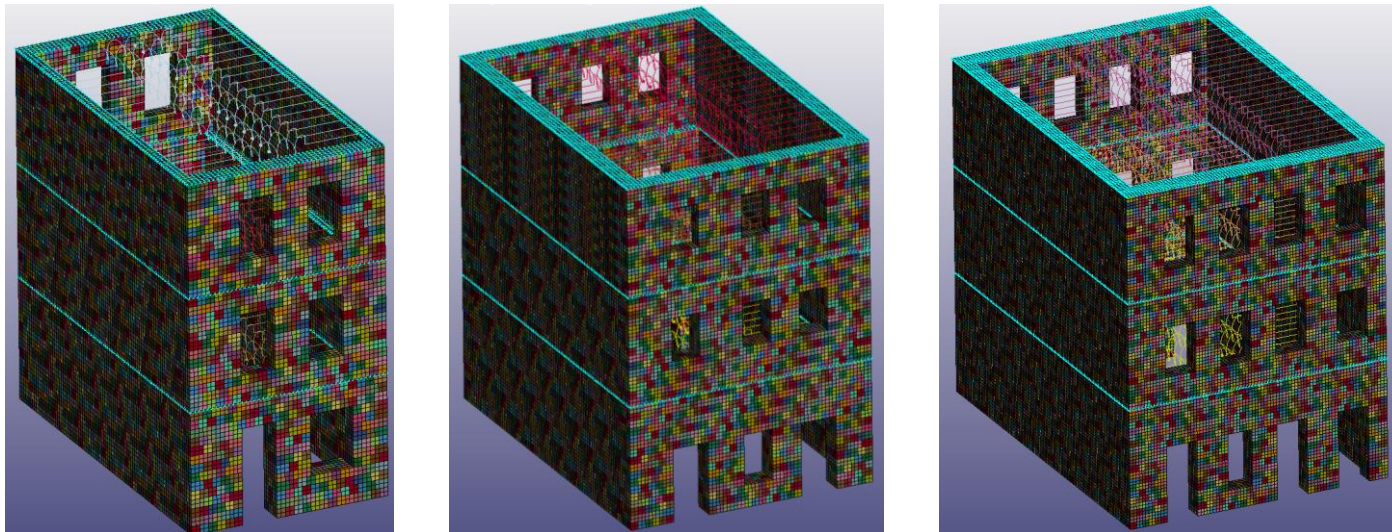
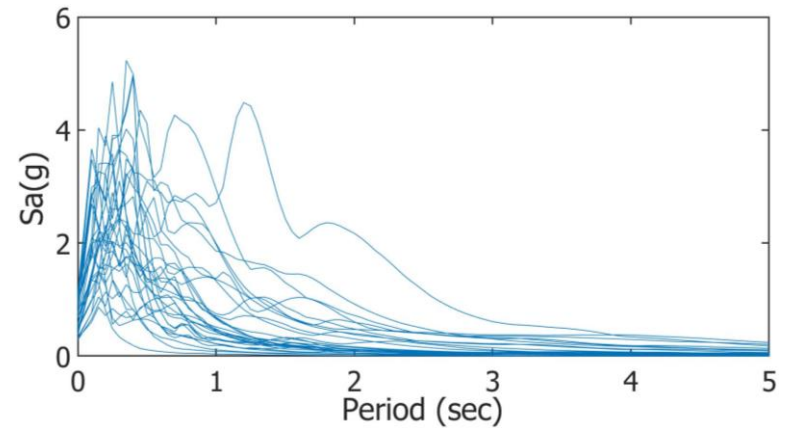


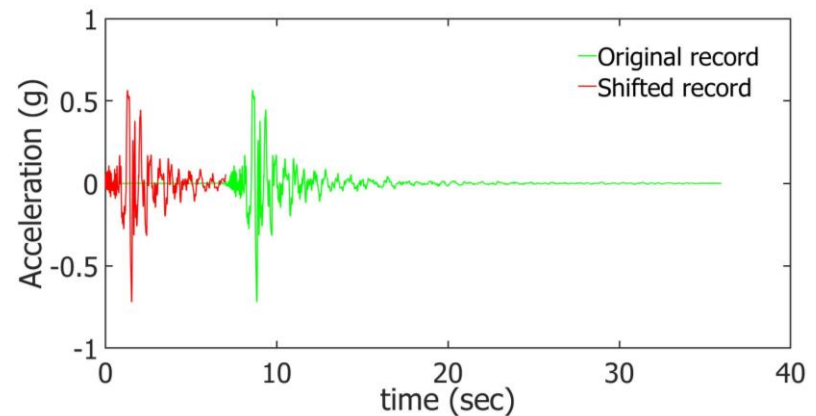
Fig. 17 Example of LS-Dyna models randomly generated

A set of 30 records were selected in accordance with the local seismicity

The records are uniformly distributed according to its PGA between 0.2 to 1.2 each 0.2 (i.e. 6 records per bin). The records were cut at 5% of the PGA in the beginning and in the end, this is to reduce the computational effort.



a)



b)

Fig. 18 a) Response spectrum for selected records b) scheme of records cut

As first advance, 4 buildings were analysed when subjected to 30 records.

Across the analysis, the technique probed to represent different levels of damage and loss volume as is shown in Fig.19.

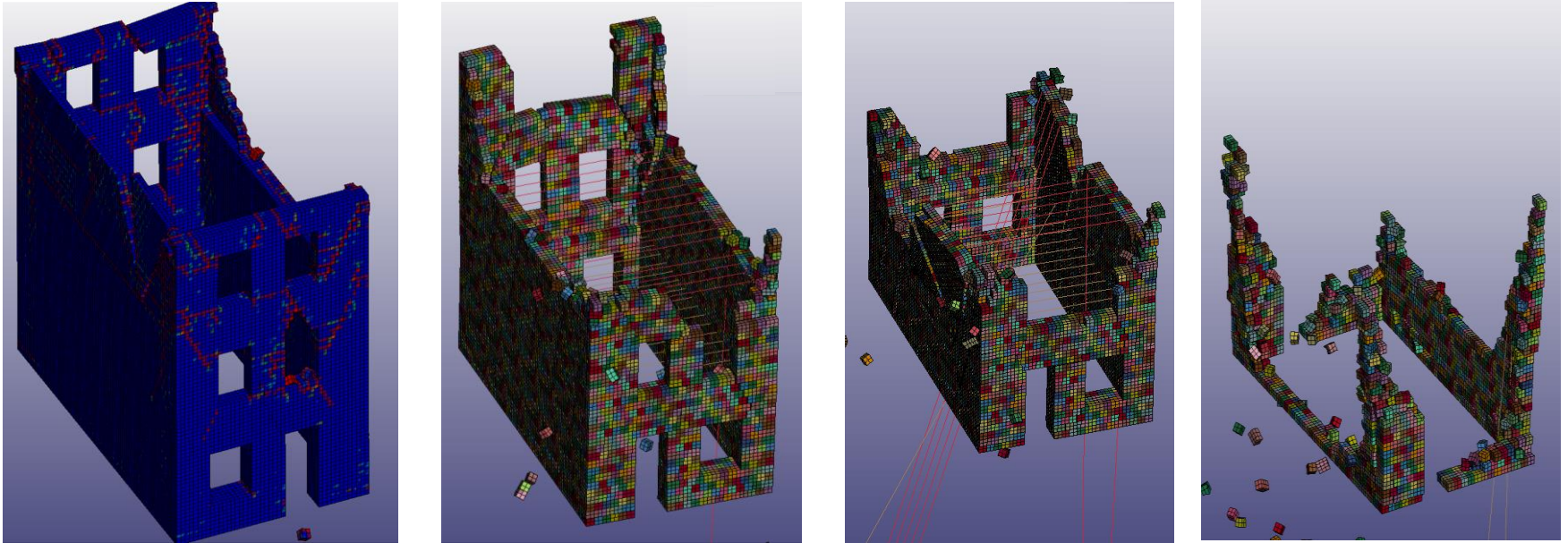


Fig. 19 Example of damage levels obtained during the analysis

The correlation coefficient (R) between loss volume and spectral acceleration was assessed for a range of periods

The R value was assessed when fitting the cloud of points “Loss volume Vs Sa” to a log normal cumulative function. The Sa at 0.6 sec was selected to plot the consequence function

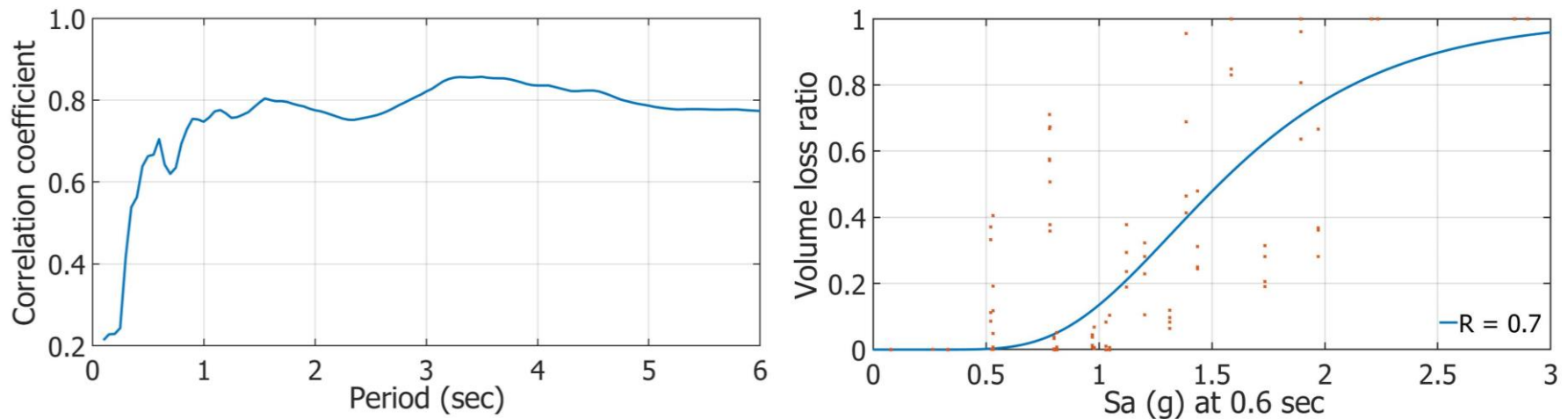


Fig. 20 a) Correlation coefficient of loss volume Vs Sa for a range of periods b) Volume loss ratio consequence function for Sa at 0.6 sec

Future research

- To perform the analysis in all the masonry portfolio
- To improve the correlation between loss volume and the intensity motion level
- To propose and model retrofitted buildings
- To perform benefit-cost analysis

Articles

- Lovon H, Silva V, Vicente R, Ferreira T, Costa A (2020). Characterization of the Masonry Building Stock in Portugal for Earthquake Risk Assessment. Engineering Structures (accepted, pending of minor revisions)

Many thanks

INFRARISK - Summer Workshop 2020